Journal of Renewable Energies
Revue des Energies Renouvelables
journal home page : https://revue.cder.dz/index.php/rer

Research Paper

# Perturb and observe maximum power point tracking method for photovoltaic systems using duty-cycle modulation

Theodore Louossi [a], Noël Djongyang [a] *, Olivier Thierry Sosso Mayi [b], Arnaud Nanfak [c]

[a] *Department of Renewable Energy, National Advanced School of Engineering of Maroua, University of Maroua PO Box 46, Maroua-Cameroon*
[b] *Department of Electrical Engineering, Higher Technical Teachers Training College of Douala, University of Douala PO Box 2701, Douala-Cameroon*
[c] *Laboratory of Energy, Materials, Modelling and Methods, National Higher Polytechnic School of Douala, University of Douala PO Box 2701, Douala-Cameroon*

ARTICLE INFO

Article history:
Received 11 July 2020
Accepted 02 December 2020

Keywords:
*Perturb and Observe,*
*Duty cycle modulation,*
*Pulse width modulation,*
*Photovoltaic system*

ABSTRACT

This paper presents the implementation of perturb and observe maximum power point tracking algorithm with Duty Cycle Modulation instead of pulse width modulator for photovoltaic power generators. Like all the different methods used for tracking the maximum power point of photovoltaic system, perturb and observe method use a Pulse Width Modulation to control the DC-DC converter. Here, the Duty Cycle Modulation is used in the place of Pulse Width Modulation. A detailed analysis of the approach is proposed and simulations are performed using MATLAB/Simulink software. The results show the performance and speed at which this control reaches the maximum power point. The response times is very low and is between 0.0125s and 0.05s depending on the climatic variations. So, Duty Cycle Modulation can be used as an alternative to Pulse Width Modulation for the search of the maximum power point.

## 1. Introduction

Due to increasing demand for energy and depletion of fossil fuel reserves, looking for alternative energy resources has become essential [1]. The renewable energies such as wind energy, photovoltaic (PV) energy present an alternative solution to produce needed electricity

* *Corresponding author, E-mail address: noeldjongyang@gmail.com*
*Tel.: +237 691328132*

ISSN: 1112-2242 / EISSN: 2716-8247

[2]. Among renewable energy resources, PV energy has drawn much attention in recent years. Nowadays, demand of PV systems is increasing rapidly due to environmentally friendly energy conversion process and the features of solar energy such as plentiful amount, free of cost, sustainable and global availability [3]. However, the power generated by PV modules depends on environmental factors, e.g. solar radiation and atmospheric temperature. These factors affect both current-voltage and power-voltage characteristics of the PV system and hence connected load. In order to reduce the impact of environmental variations, a Maximum Power Point tracking (MPPT) controller is required to optimally exploit the available power [4].

Many MPPT technics have been proposed for tracking the maximum power point (MPP) of PV systems such as perturb and observe (P&O) [5-6-7-8], Incremental conductance (INC) [6-8], Hill climbing [8], Fractional open circuit voltage (FOCV) [8], Fractional Short-Circuit Current (FSCC) [8], fuzzy logic [3-4-8] and neutral network [4-8]. In practice, P&O method is the technic most commonly used due to its low cost, ease of implementation and relatively good tracking performance, compared to other technics [9].

All MPPT controls techniques are used to produce a duty cycle automatically and a DC-DC power stage is connected with MPPT controls to allow a PV generator produce the maximum persistent power, at any value of the metrological terms or the change in the values of loads which can happen at any moment [10]. The duty cycle produced by the MPPT algorithms is converted into a DC-DC control signal using the PWM technique. In this paper, we propose to use the duty cycle modulation (DCM) technique instead of the PWM technique. The DCM is a class of signal conversion techniques in which an input signal $x$ is transformed into a train of switching wave where pulse width and period of the modulated signal vary simultaneously as function of modulating signal [11-12]. Both DCM and PWM are modulation techniques that transform a modulating signal into a pulse train. The difference between the two is that in DCM, the frequency varies according to the modulating signal which is not the case in PWM where the frequency is fixed**.** Numerous studies have shown that it offers more advantages than the traditional PWM strategy in several application areas such as analogical-to-digital conversion [13-14], digital-to-analogical conversion [15], power electronic drivers [16-17], digital transmission systems for arbitrary waveforms, power quality [18], and optical transmission [19]. The aim of this work is to make an implementation of perturb and observe maximum power point tracking algorithm with DCM.

After the Introduction section, the PV system configuration used for the study is presented in section 2. Section 3 is devoted to a brief description of non-inverter duty cycle modulation.

Section 4 includes simulation results and discussion. Finally, a conclusion is presented in section 5.

## 2. PV system configuration

Figure 1 illustrates the configuration of PV power system with MPPT stage.

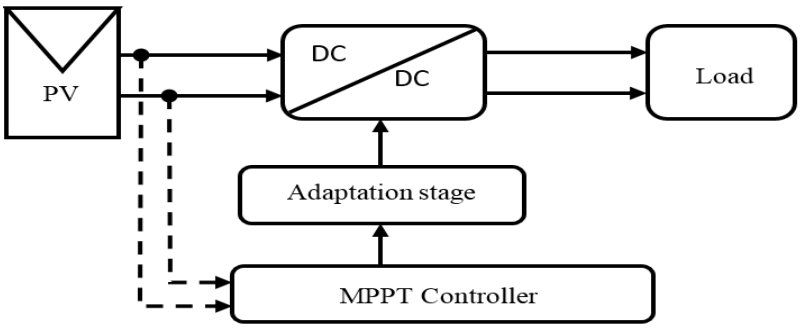


Fig 1: Configuration of PV power system with MPPT stage

The PV power system contains a solar array, a DC-DC power converter connected directly to the load, an MPPT controller and an adaptation stage located between the MPPT controller and the DC-DC power converter.

### 2.1 Solar cell and PV module

The solar cell is the basic unit of a PV panel and it is the element in charge of transforming the sun rays or photons directly into electric power by a process called “photovoltaic effect” [9-15]. The figure 2: shows the equivalent circuit of solar cell. The model chosen is composed of a current source resulting from the luminous flux, a simple diode which describes the polarization phenomenon and a resistance to materialize the losses here. The symbols used in the model are summarized in nomenclature:

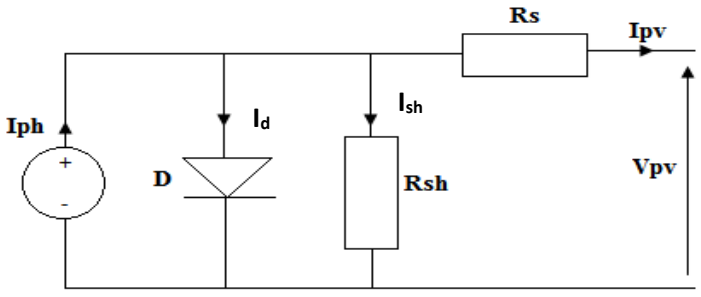


Fig 2: Equivalent circuit of solar cell [21]

In Fig. 2, by applying Kirchhoff's current law where $I_{ph}$ is Photovoltaic current source, $I_d$ is Diode current, $I_{sh}$ is Shunt current and output current of PV cell ($I_{pv}$ ) can be expressed by equation (1).

$$I_{pv} = I_{ph} - I_d - I_{sh} \tag{1}$$

The photo-current is proportional to solar irradiation G in W/m² and can be expressed by:

$$I_{ph} = \left(\frac{G}{G_r}\right)\left(I_{scr} + k_i\left(T - T_r\right)\right) \tag{2}$$

Where

$I_{scr}$ is short-circuit current of the PV module at standard test condition (STC) of 25°C and 1000 W/m², $k_i$ is temperature coefficient of short-circuit, $T$ is cell temperature (K), $T_r$ is reference temperature (K) and $G_r$ is reference solar irradiation (W/m²).

The diode current is given by:

$$I_d = I_s\left(\exp\left(\frac{q\left(V_{pv} + R_s I_{pv}\right)}{nK_b T}\right) - 1\right) \tag{3}$$

where

$I_s$ is diode saturation current, $q$ is electron's charge, $n$ is the diode ideality factor and $K_b$ is Boltzmann's constant. $I_s$ can be expressed by equation (4)

$$I_s = I_{rs}\left(\frac{T}{T_r}\right)^3 \exp\left(\frac{qE_g}{nK_b}\left(\frac{1}{T_r} - \frac{1}{T}\right)\right) \tag{4}$$

where

$I_{rs}$ is the diode saturation current at $T_r$, $E_g$ is the silicon gap energy of semiconductor. $I_{sr}$ and is given by equation (5)

$$I_{rs} = \frac{I_{scr}}{\exp\left(\frac{qV_{oc}}{nK_b T} - 1\right)} \tag{5}$$

where

$V_{oc}$ is the open-circuit voltage. The shunt current is given by equation(6),

$$I_{sh} = \frac{V_{pv} + R_s I_{pv}}{R_{sh}} \tag{6}$$

For $N_S$ cells in series and $N_P$ cells in parallel, the characteristic of a PV module is delivered as below [1]:

$$I_{pv} = N_p I_{ph} - N_p I_s \left( \exp\left( \frac{q\left(V_{pv} + R_s I_{pv}\right)}{N_s n K_b T} \right) - 1 \right) - \frac{V_{pv} + R_s I_{pv}}{R_{sh}} \quad (7)$$

2.2 DC-DC power converter

DC-DC converter is an electronic circuit which converts a source of direct current from one voltage level to another [6]. We adopt a boost converter as the DC-DC power converter. It is widely used as DC-DC converter for photovoltaic application owing to its simple circuit and system design, high conversion efficiency and reduced voltage stress [7]. Its circuit topology is presented in figure 3: It is composed of switching devices, inductors and capacitors.

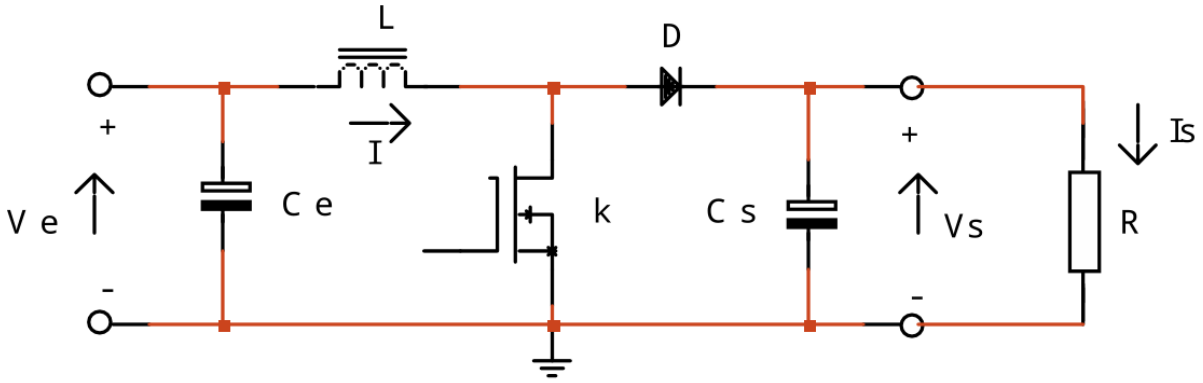


Fig 3: Topology circuit of DC/DC boost converter

$V_e = V_{pv}$ is the input voltage and $V_s$ is the output voltage of the boost converter. The output voltage is greater than the input voltage and is expressed as [4]:

$$V_s = \frac{V_{pv}}{1-\alpha} \quad (8)$$

Where $\alpha$ is the duty cycle in interval [0; 1]

We assume that the inductor current $i_L$ is equal to PV current $I_{pv}$. The switch is usually an IGBT or MOSFET [1]. The passive components $R$, $L$, $C_e$ and $C_s$ are converter load, inductor, input and output capacitor, respectively.

2.3 P&O MPPT algorithm

The perturb and observe MPPT algorithm is probably the most frequently used in practice, mainly due to its easy implementation [20]. As the name suggest, the P&O algorithm works on idea of introducing perturbation to the system's operating point to generate maximum output

power. The principle of this algorithm is to disturb the voltage of the PV panel while acting on the duty cycle $\alpha$. Indeed, following this disturbance, the power supplied by the PV panel at time $k$ is calculated, then compared to the previous one at time $(n-1)$. If the power increases, the MPP is approached and the duty cycle variation is maintained in the same direction. On the contrary, if the power decreases, we move away from the MPP. Then we have to reverse the direction of the change in the duty cycle [22]. The figure 4 shows the flowchart of this algorithm, it can be resumed as following:

First, the voltage $V_{pv}(n)$ and current $I_{pv}(n)$ are measured for calculating the power $P_{pv}(n)$. The variations of power $\Delta P_{pv} = P_{pv}(n) - P_{pv}(n-1)$ and of voltage $\Delta V_{pv} = V_{pv}(n) - V_{pv}(n-1)$ are calculated.

- If $\Delta P_{pv} \times \Delta V_{pv} > 0$, the duty cycle $\alpha(n+1) = \alpha(n) + \Delta\alpha$
- If $\Delta P_{pv} \times \Delta V_{pv} < 0$, the duty cycle $\alpha(n+1) = \alpha(n) - \Delta\alpha$

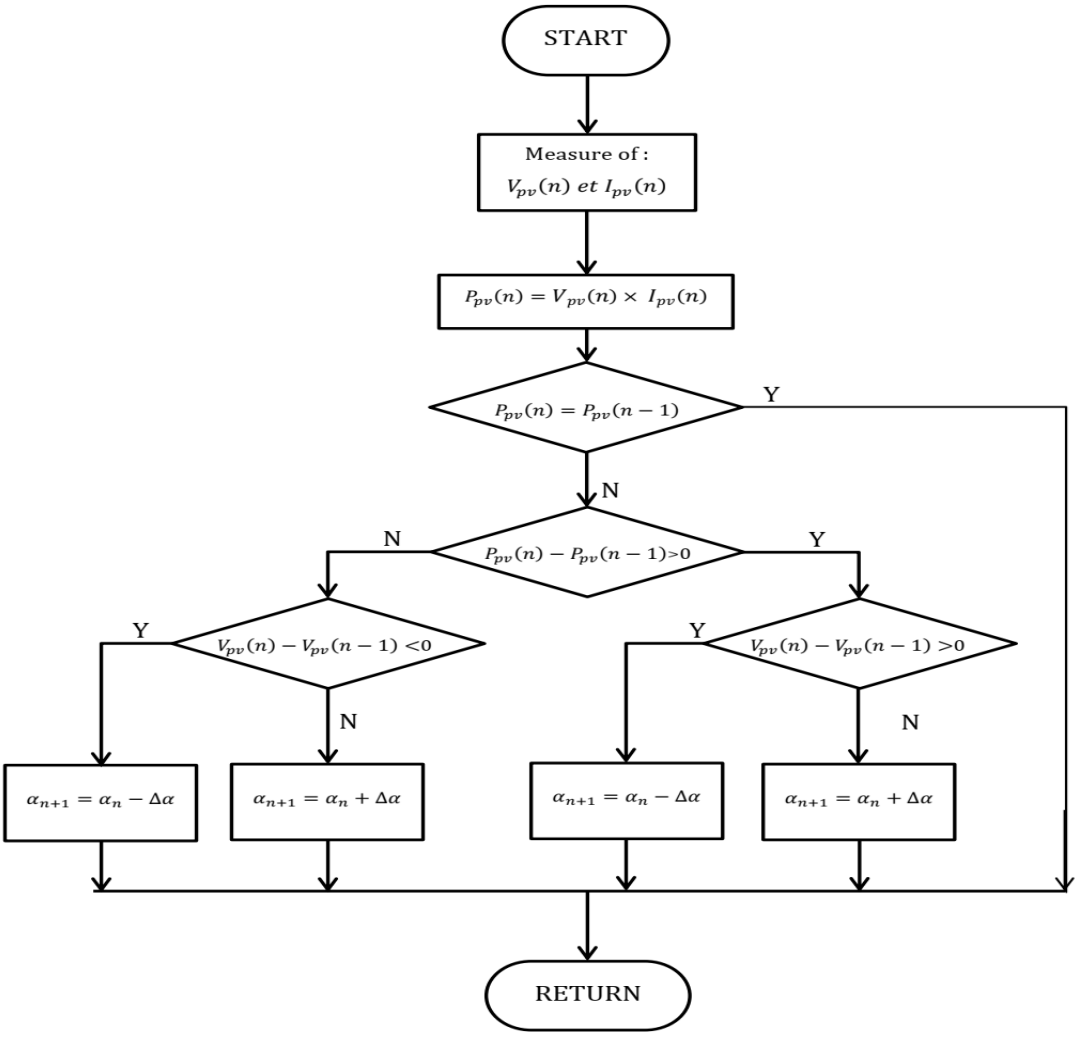


Fig 4: Flow chart of P&O algorithm [22]

## 3. Duty Cycle Modulation technic

Initially invented and patented by Biard et al. in 1962, the realization of classical DCM circuit requires at least two integrated circuits and seven passive elements [23]. New simpler and higher quality duty cycle modulators have subsequently been proposed by Mbihi et al. Initially proposed for instrumentation problems, they are today used in many sectors such as optical transmission and analogic-to-digital conversion. The scheme of the DCM developed by Mbihi et al is shown in figure 5: The symbols used in the model are summarized in nomenclature.

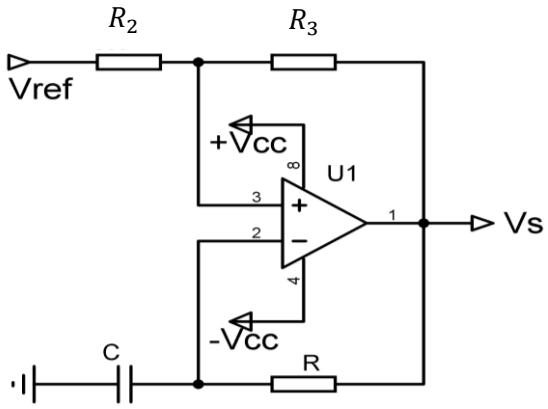


Fig 5: Structure of the DCM

This modulator has the advantage of being simpler than a PWM modulator. Its period $T_s$ and duty cycle $\alpha$ are defined by [24]:

$$T_s = RC \ln\left(\frac{(\alpha_2 x)^2 - ((\alpha_1+1)V_{sat})^2}{(\alpha_2 x)^2 - ((\alpha_1-1)V_{sat})^2}\right) \tag{9}$$

$$\alpha = \frac{\ln\left(\dfrac{\alpha_2 V_{ref} - (\alpha_1+1)V_{sat}}{\alpha_2 V_{ref} - (\alpha_1-1)V_{sat}}\right)}{\ln\left(\dfrac{(\alpha_2 V_{ref})^2 - ((\alpha_1+1)V_{sat})^2}{(\alpha_2 V_{ref})^2 - ((\alpha_1-1)V_{sat})^2}\right)} \tag{10}$$

with

$$\begin{cases} \alpha_1 = \dfrac{R_1}{R_1+R_2} \\ \alpha_2 = \dfrac{R_2}{R_1+R_2} \end{cases} \tag{11}$$

Its minimum or central period and duty cycle (for $V_{ref} = 0\,\text{V}$) are given by:

$$\begin{cases} T_0 = 2RC\ln\left(1+2\dfrac{R_1}{R_2}\right) \\ \alpha = \dfrac{1}{2} \end{cases} \tag{12}$$

The figure 6 and 7 show the evolution of the duty cycle and frequency as a function of the control voltage for different resistance values $R_2$. They show the impact of the resistor $R_2$ in the relationship between the modulating signal and the value of the duty cycle on the one hand (figure 6) and the modulating signal and frequency on the other hand (figure 7). Although frequency variation could be seen as a problem, this is basically not the case, since the range of frequency variation as a function of the modulating signal is known (figure 7), so the dimensioning is done accordingly. It should be noted that in the DCM the center frequency (maximum i.e. for x=0) is the frequency to be taken into account when sizing the components of the DCM modulator.

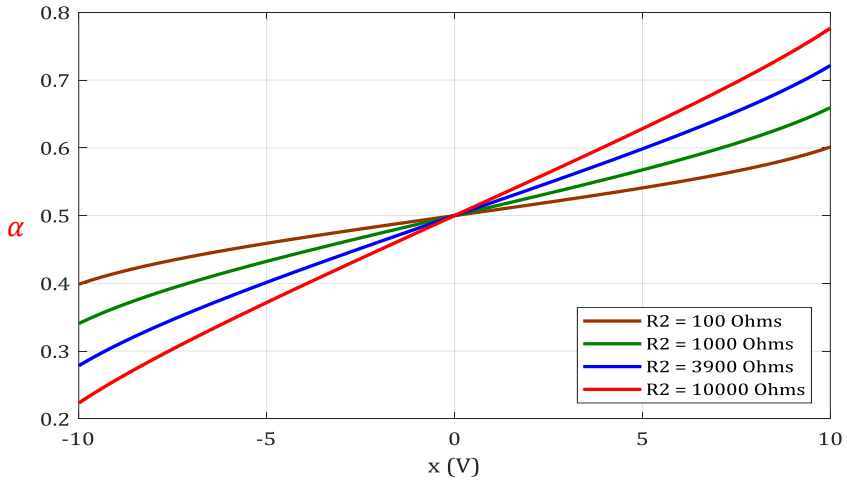


Fig 6: Duty-cycle of a non-inverting DCM with a variable control

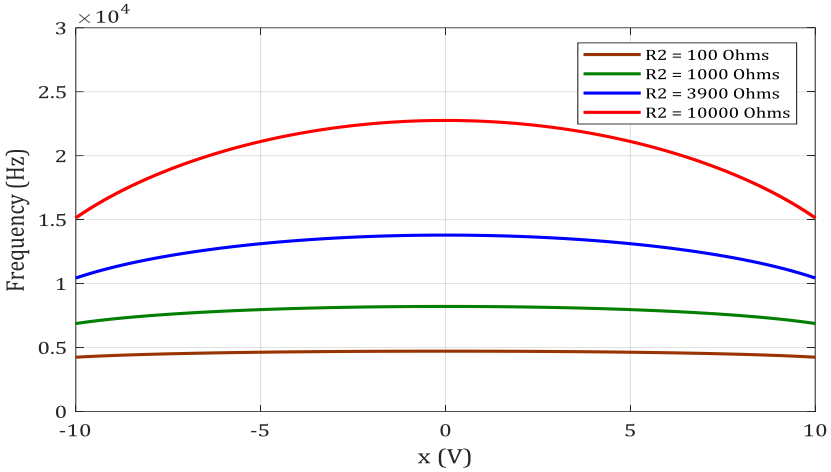


Fig 7: Frequency of a non-inverting DCM with a variable control

## 4. Results and discussion

The MATLAB/Simulink platform is shown in Fig 8: The duty cycle produced by the perturb and observe by algorithm is injected into the DCM block, which calculates the control voltage of duty cycle modulator for equation 10. The output signal of the non-inverting duty cycle modulator is then used to control the switch of the DC-DC stage.

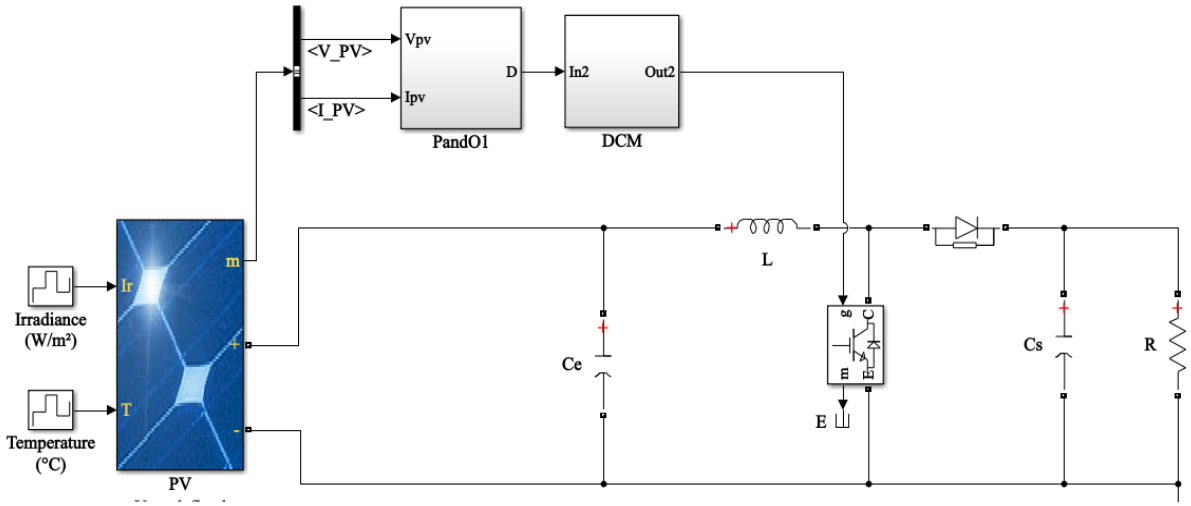


Fig 8: Simulink model

The parameters of the boost converter, P&O MPPT algorithm and duty cycle modulation are listed in table 1, table 2 and table 3 respectively.

Table 1: Parameters of boost converter

| Parameters | Values |
|---|---|
| Inductance $L$ | 3 mH |
| Input filter capacitance $C_e$ | 100 µF |
| output filter capacitance $C_s$ | 100 µF |
| Load $R$ | 30 Ω |

Table 2: Parameters of the P&O MPPT algorithm

| Parameters | Values |
|---|---|
| Initial duty cycle $\alpha_{init}$ | 0.42 |
| maximum duty cycle $\alpha_{\max}$ | 0.8 |
| minimum duty cycle $\alpha_{\min}$ | 0.08 |
| Increment value $\Delta\alpha$ | 5e-6 |

Table 3: Parameters of duty-cycle modulator

| Parameters | Values |
|---|---|
| $R$ | $1\ k\Omega$ |
| $R_2$ | $10\ k\Omega$ |
| $R_3$ | $4.8\ k\Omega$ |
| $C$ | $1\ nF$ |
| $V_{sat}$ | $12\ V$ |

4.1 Simulation of PV module

PV module used in this work is a 60W PV panel used in [24]. The data sheet of the reference model under standard test conditions is given in table 4. The frequency of simulation is $10kHz$. Figures 9 and 10 represent the different solar radiation and temperature profile used for simulation. Figures 11.a and 12.a represent P-V and I-V characteristics with different irradiations (1kW/m$^2$, 0.75kW/m$^2$, 0.50kW/m$^2$ and 0.25kW/m$^2$) at a constant temperature fixed at 25°C; while figures 11.b and 12.b represent P-V and I-V characteristics with different ambient temperatures (0°C, 25°C, 50°C and 75°C) at a constant solar irradiation fixed at 1000 W/m². We notice that the power output characteristic of PV system is non-linear and crucially

influenced by solar irradiation and temperature with more influence of irradiation on the short-circuit current than the influence of temperature on the open-circuit voltage.

Table 4: Specifications of the PV module

| Name | Unity | Parameters | Value |
|---|---|---|---|
| Maximum power | W | $P_m$ | 60.53 |
| Maximum power voltage | V | $V_m$ | 17.05 |
| Maximum power current | A | $I_m$ | 3.55 |
| Open circuit voltage | V | $V_{oc}$ | 21.1 |
| Short circuit current | A | $I_{sc}$ | 3.8 |
| N° of cell in a module | - | $N_s$ | 36 |
| Ideal factor of diode | - | $n$ | 1.3 |
| Series resistance | Ω | $R_s$ | 0.5 |
| Shunt resistance | Ω | $R_{sh}$ | 124.8 |
| Temperature coefficient of | - | $V_{oc}$ | -0.229 |
| Temperature coefficient of | - | $I_{sc}$ | 0.0307 |

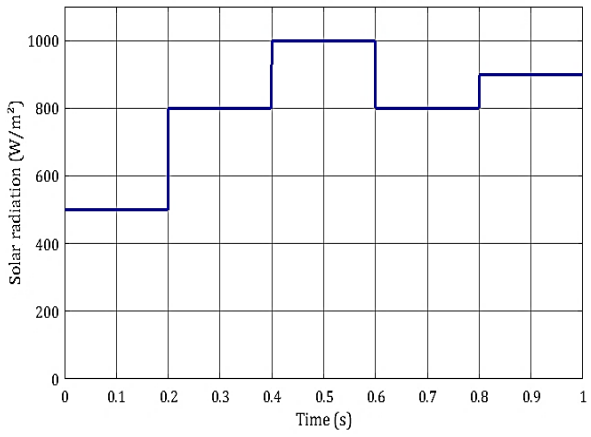


Fig 9: Solar radiation profile used for simulation

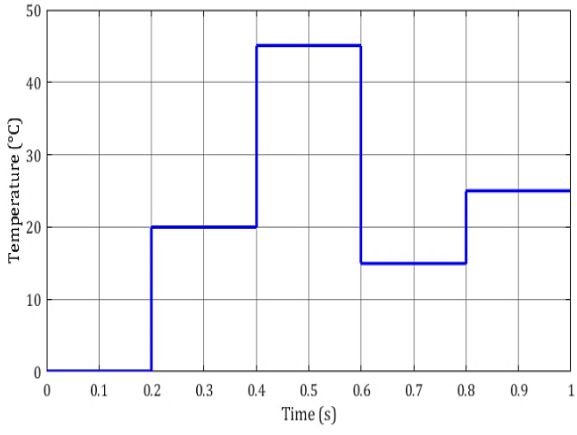


Fig 10: Temperature profile used for simulation

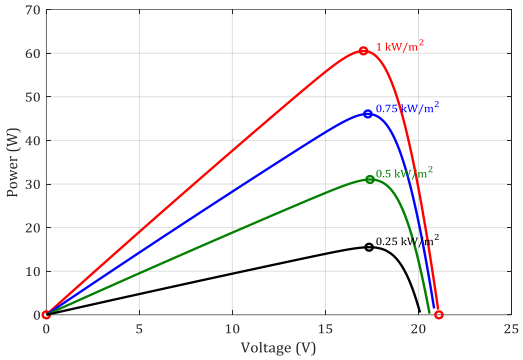


(a) At different solar radiations

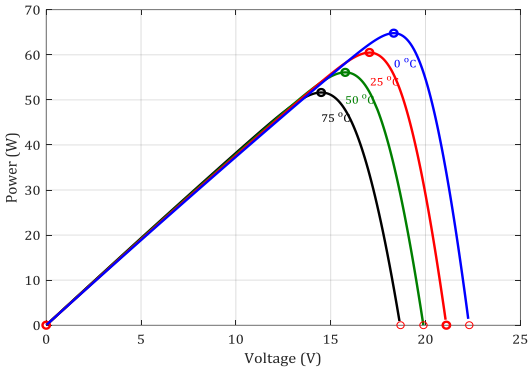


(b) At different ambient temperatures

Fig 11: P-V characteristics

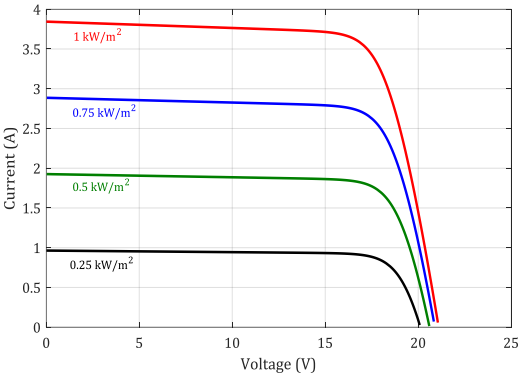


(a) At different solar radiations

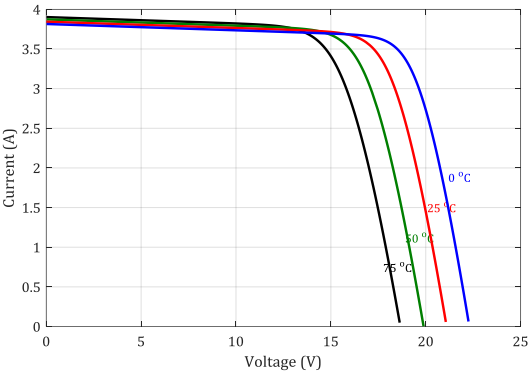


(b) At different ambient temperatures

Fig 12: I-V characteristics

## 4.2 Simulation and results analysis of P&O MPPT

The results of P&O MPPT algorithm using the DCM technics for PV system operated under standard environmental conditions (figure 14), under variable irradiations (figure 15) and under variable temperatures (figure 16) are presented in this section. The parameters of duty cycle modulators use for simulation are listed in table 3 and the Simulink bloc in figure 13.

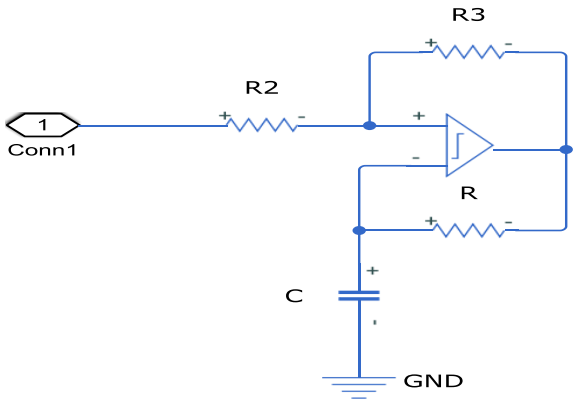


Fig 13: DCM Simulink bloc

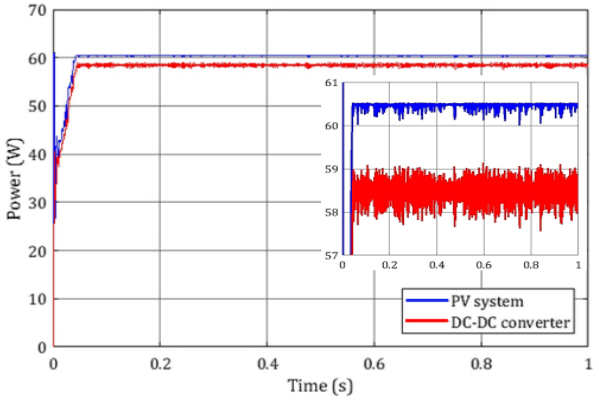


(a) Powers for standard condition

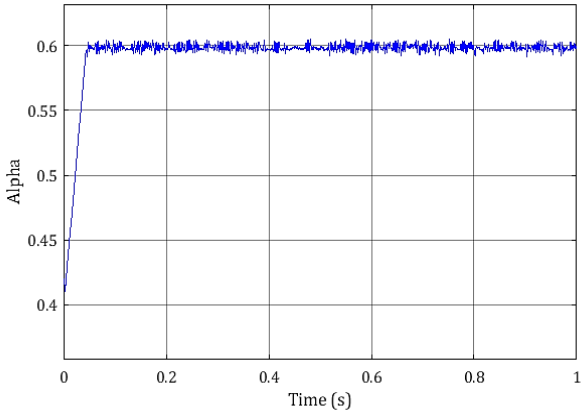


(b) Duty cycle for standard condition

Fig 14: Results for standard environmental conditions

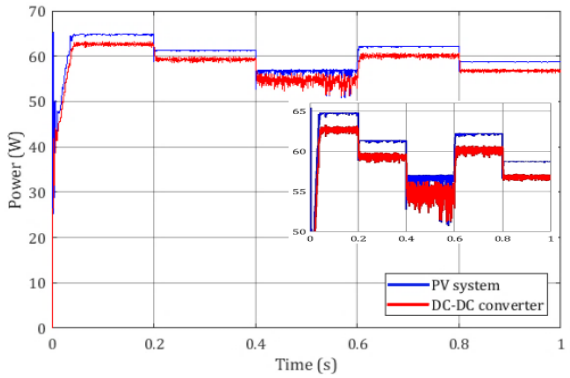


(a) Powers for variable irradiation

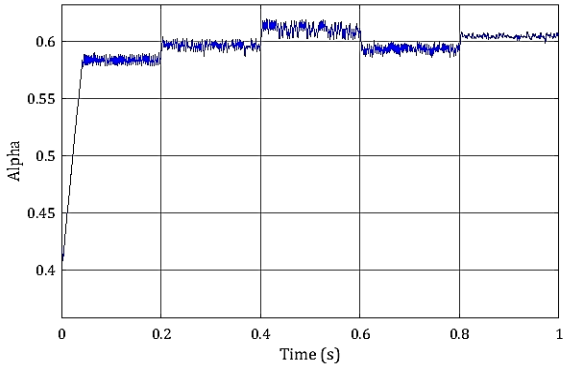


(b) Duty cycle for variable irradiation

Fig 15: Results for constant temperature and variable irradiation

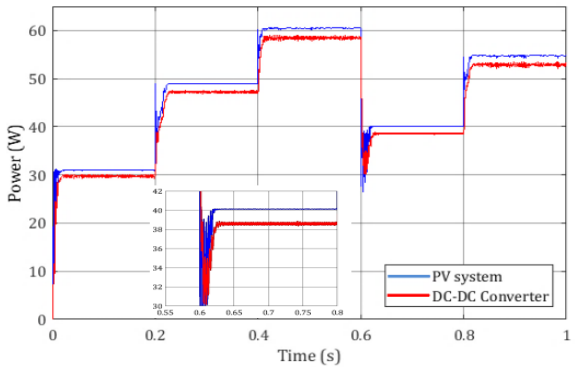


(a) Powers for variable temperature

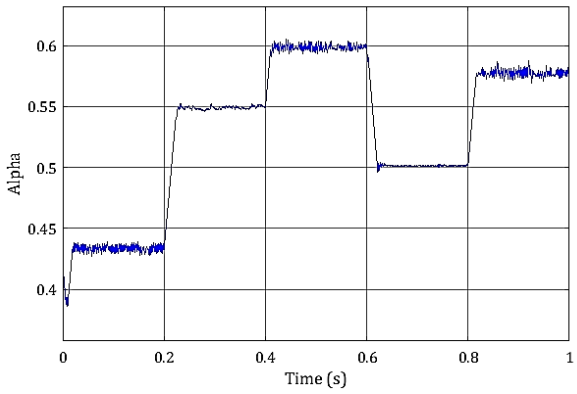


(b) Duty cycle for variable temperature

Fig 16: Results for constant irradiation and variable temperature

The results obtained in the standard environmental conditions show that the output power of the PV system oscillates less than 0.5 W. On the other hand, the output power of the DC-DC chopper shows oscillations in the order of 1 W. The reaction time of the MPPT algorithm using DCM is less than 0.05 s. The curves in figure 14 show the behaviour of the system in cases of variations of irradiation. Regarding the power curve, the same oscillations of the output power of the PV system are observed for constant ranges of irradiation. During the transition phases of the irradiation, the output power of the PV system quickly follows the maximum power point with response times of less than 0.05s. The same behaviour in response time due to irradiation changes is observed with the output power of the DC-DC converter. For temperature variations, the steady state corresponding to constant temperature values show similar behaviour to that obtained at standard environmental conditions, i.e. oscillations of less than 0.5W and 1W for the PV system and DC-DC converter, respectively. In terms of reaction time following temperature transitions, the system has a response time of less than 0.025s.

## 5. Conclusion

The main aim of this work was to show that it is possible to use the Duty Cycle Modulation technique for maximum power point tracking purposes in photovoltaic systems. results obtained under standard environmental conditions and under variable temperature and irradiations conditions show that the P&O MPPT algorithm using DCM effectively allows firstly to extract the maximum power from the PV system and secondly to have low oscillations at the outputs of the PV system and the DC-DC converter. These results are satisfactory and show that DCM can be used as an alternative to PWM.

## Nomenclatures

| Parameters | Name | unity |
|---|---|---|
| $I_{ph}$ | Photovoltaic current source | $A$ |
| $I_d$ | Diode current | $A$ |
| $I_{sh}$ | Shunt current | $A$ |
| $R_{sh}$ | Shunt resistance | Ω |
| $R_s$ | Series resistance | Ω |
| $I_{pv}$ | Cell current | $A$ |
| $V_{pv}$ | Cell voltage | V |
| $R, R_2, R_3$ | Resistors | Ω |
| C | Capacitor | $F$ |
| $U_1$ | Integrated circuit (Operational amplifier) | |

## 6. References

[1] R. Khanaki, M. A. M. Radzi, and M. H. Marhaban, ‘Comparison of ANN and P&O MPPT methods for PV applications under changing solar irradiation’, in 2013 IEEE Conference on Clean Energy and Technology (CEAT), Lankgkawi, Malaysia, Nov. 2013, pp. 287–292, doi: 10.1109/CEAT.2013.6775642.

[2] A. Kchaou, A. Naamane, Y. Koubaa, and N. K. M’Sirdi, ‘Comparative study of different MPPT techniques for a stand-alone PV system’, in 2016 17th International Conference on Sciences and Techniques of Automatic Control and Computer Engineering (STA), Sousse, Tunisia, Dec. 2016, pp. 629–634, doi: 10.1109/STA.2016.7952092.

[3] R. Kumar, B. Kumar, and S. D, ‘Fuzzy Logic based Improved P&O MPPT Technique for Partial Shading Conditions’, in 2018 International Conference on Computing, Power and Communication Technologies (GUCON), Greater Noida, Uttar Pradesh, India, Sep. 2018, pp. 775–779, doi: 10.1109/GUCON.2018.8674917.

[4] L. Bouselham, B. Hajji, and H. Hajji, ‘Comparative study of different MPPT methods for photovoltaic system’, in 2015 3rd International Renewable and Sustainable Energy Conference (IRSEC), Marrakech, Morocco, Dec. 2015, pp. 1–5, doi: 10.1109/IRSEC.2015.7455085.

[5] T. Selmi, M. Abdul-Niby, L. Devis, and A. Davis, ‘P&O MPPT implementation using MATLAB/Simulink’, in 2014 Ninth International Conference on Ecological Vehicles and Renewable Energies (EVER), Monte-Carlo, Mar. 2014, pp. 1–4, doi: 10.1109/EVER.2014.6844065.

[6] F. E. Tahiri, K. Chikh, M. Khafallah, and A. Saad, ‘Comparative study between two Maximum Power Point Tracking techniques for photovoltaic system’, in 2016 International Conference on Electrical and Information Technologies (ICEIT), May 2016, pp. 107–112, doi: 10.1109/EITech.2016.7519571.

[7] J. K. Udavalakshmi and M. S. Sheik, ‘Comparative Study of Perturb & Observe and Look -Up Table Maximum Power Point Tracking Techniques using MATLABISimulink’, in 2018 International Conference on Current Trends towards Converging Technologies (ICCTCT), Coimbatore, Mar. 2018, pp. 1–5, doi: 10.1109/ICCTCT.2018.8550835.

[8] B. Subudhi and R. Pradhan, ‘A Comparative Study on Maximum Power Point Tracking Techniques for Photovoltaic Power Systems’, IEEE Trans. Sustain. Energy, vol. 4, no. 1, pp. 89–98, Jan. 2013, doi: 10.1109/TSTE.2012.2202294.

[9] M. A. Abdourraziq, M. Ouassaid, M. Maaroufi, and S. Abdourraziq, 'Modified P&O MPPT technique for photovoltaic systems', in 2013 International Conference on Renewable Energy Research and Applications (ICRERA), Madrid, Spain, Oct. 2013, pp. 728–733, doi: 10.1109/ICRERA.2013.6749849.

[10] D. Haji and N. Genc, 'Fuzzy and P&O Based MPPT Controllers under Different Conditions', in 2018 7th International Conference on Renewable Energy Research and Applications (ICRERA), Paris, Oct. 2018, pp. 649–655, doi: 10.1109/ICRERA.2018.8566943.

[11] Y. Paulin, D. Sounsoumou, Haman-Djalo, J. Mbihi, and J. Yves Effa, 'Modélisation et simulation virtuelle d'un nouveau schéma de réglage de hacheurs Boost à commande rapprochée par modulation en rapport cyclique', pp. 176–185, Jan. 2017.

[12] L. N. Nneme and J. Mbihi, 'Modeling and Simulation of a New Duty-Cycle Modulation Scheme for Signal Transmission Systems', American Journal of Electrical and Electronic Engineering, vol. 2, no. 3, pp. 82–87, Jan. 2014, doi: 10.12691/ajeee-2-3-4.

[13] Paul Owondi Etouke and al, 'An optimal control scheme for a class of Duty Cycle Modulation Buck choppers : Analog Design and virtual simulation' Journal of Electrical Engeneering, Control and Computer Science-JEEECCS in 2020, volume 6, Issue 19, pages 13-20.

[14] G. Sonfack, J. Mbihi, and B. L. Moffo, 'Optimal Duty-Cycle Modulation Scheme for Analogic-To-Digital Conversion Systems', International Journal of Electronics and Communication Engineering, vol. 11, no. 3, pp. 354–360, Jan. 2018.

[15] B. L. Moffo, J. Mbihi, L. N. Nneme, and M. Kom, 'A novel digital-to-analogic conversion technique using duty-cycle modulation', International Journal of circuits, systems and signal processing, vol. 7, no. 1, pp. 42–49, 2013.

[16] J. Mbihi and L. Nneme, 'A novel control scheme for buck power converters using duty-cycle modulation', IJPELEC, vol. 5, no. 3/4, p. 185, 2013, doi: 10.1504/IJPELEC.2013.057038.

[17] D. Sounsoumou, Y. Paulin, J. Mbihi, H. Djalo, and E. Joseph, 'Virtual Digital Control Scheme for a Duty-Cycle Modulation Boost Converter', Aug. 2018.

[18] T. P. N. Nna, S. N. Essiane, and S. P. Ngoffé, 'Control of an Active Filter by Duty Cycle Modulation (DCM) for the Harmonic Decontamination of a Three-Phase Electrical Network', Journal of Power and Energy Engineering, vol. 8, no. 7, Art. no. 7, Jul. 2020, doi: 10.4236/jpee.2020.87001.

[19] L. T. Nguefack, F. Pauné, G. W. Kenfack, and J. Mbihi, 'A Novel Optical Fiber Transmission System Using Duty-Cycle Modulation and Application to ECG Signal: Analogic Design and Simulation', Journal of Electrical Engineering, Electronics, Control and Computer Science, vol. 6, no. 3, Art. no. 3, Jun. 2020.

[20] N. Drir, L. Barazane, and M. Loudini, 'Comparative study of maximum power point tracking methods of photovoltaic systems', in 2014 International Conference on Electrical Sciences and Technologies in Maghreb (CISTEM), Tunis, Tunisia, Nov. 2014, pp. 1–5, doi: 10.1109/CISTEM.2014.7077055.

[21] B. Lekouaghet, A. Boukabou, N. Lourci, and K. Bedrine, 'Control of PV grid connected systems using MPC technique and different inverter configureuration models', Electric Power Systems Research, vol. 154, pp. 287–298, Jan. 2018, doi: 10.1016/j.epsr.2017.08.027.

[22] A. Nanfak, 'Etude et élaboration d'un mini-superviseur de sources d'énergie électrique hybrides réseau/solaire pour l'alimentation d'un conditionneur air', Thesis, Douala, 2015.

[23] J. R. Biard, 'Duty cycle modulated multivibrator', US3037172A, May 29, 1962.

[24] V. K. Viswambaran, A. Ghani, and E. Zhou, 'Modelling and simulation of maximum power point tracking algorithms & review of MPPT techniques for PV applications', in 2016 5th International Conference on Electronic Devices, Systems and Applications (ICEDSA), Ras Al Khaimah, Dec. 2016, pp. 1–4, doi: 10.1109/ICEDSA.2016.7818506.